Engineering Structures 56 (2013) 555–566

Contents lists available at SciVerse ScienceDirect

Engineering Structures

journal homepage: www.elsevier.com/locate/engstruct

External jacket of FRP wire for confining concrete and its advantages

Eunsoo Choi [a,1], Jong-Su Jeon [b,*], Baik-Soon Cho [c], Kyoungsoo Park [d]

[a] Department of Civil Engineering, Hongik University, Seoul 121-791, Republic of Korea
[b] School of Civil and Environmental Engineering, Georgia Institute of Technology, Atlanta, GA 30332, USA
[c] Department of Civil Engineering, CTRC, Inje University, Kimhae 621-749, Republic of Korea
[d] School of Civil and Environmental Engineering, Yonsei University, Seoul 120-749, Republic of Korea

ARTICLE INFO

Article history:
Received 22 October 2012
Revised 10 May 2013
Accepted 12 May 2013

Keywords:
FRP wires
Concrete confinement
Seismic retrofit
Stiffness ratio
Confinement ratio

ABSTRACT

This study investigates the effectiveness of FRP wire to confine concrete. For this purpose, axial compressive tests are conducted with three parameters, peak strength of concrete, confining amount of FRP wire, and epoxy application. The behavior of the FRP-wire confined concrete is examined in the axial and circumferential directions as well as in terms of volumetric strain. Each behavior is discussed according to the stiffness ratio of the confining FRP wire to concrete. Moreover, the confinement effectiveness of the FRP wire is estimated using the actual rupture strain of the FRP wire as well as the ultimate tensile strain. Both cases show slightly larger effectiveness than that of FRP sheet confined concrete. The external jacket of the FRP wire increases the peak strength satisfactory and restrains volumetric expansion when the stiffness ratio of the jacket is sufficiently large. The failure of the FRP wire confined concrete occurs at the mid-height of the cylinder. Furthermore, this study investigates the behavior of partially confined concrete exhibiting smaller peak strength compared to the corresponding fully confined specimen, as it appears to have a smaller stiffness ratio.

1. Introduction

External jackets using steel plates initially showed good performance in terms of increasing the displacement ductility and flexural strength of lap-spliced reinforced concrete (RC) columns [1,2]. However, the installation method of the steel jacket was somewhat inconvenient due to the requirement of grouting to fill up the gap between steel and concrete. Moreover, the grouting increased the cross-sectional area at the jacketed region and the dynamic characteristics of the jacketed structure were disturbed relative to the as-built structure. Jackets using fiber reinforced polymer (FRP) sheets or tubes subsequently came to the forefront as an alternative to the steel jacket on the basis of several relative benefits. The strong points of the FRP jacket are that it does not increase the cross-sectional area and a multiple layered jacket is available. However, an adhesive should be used to bond the FRP sheet to the concrete surface or another FRP sheet. This process is usually conducted manually, and tight attachment is not guaranteed. Perfect attachment of the FRP sheet on the concrete is one of the critical factors to induce immediate causing the confining pressure of the FRP sheet against the bulge of concrete.

Harries and Carey [3] conducted experimental tests to examine the effect of the gap between the concrete and the jacket on the behavior of confined concrete. They carried out compressive tests of concrete cylinders with a gap between the concrete and the jacket and compared them to the results with those obtained for a case without a gap. In the test, the gap was built by wrapping typical plastic wrap used in the kitchen. The effect of the gap was that the peak strength as a function of lateral strain appeared early. The measured lateral strain on the jacket did not represent the bulge of the concrete inside, given that the jacket did not dilate immediately according to the bulge inside the concrete due to the gap.

Several prestressing techniques have been introduced to overcome this problem. However, the prestressing methods are not easily applied to RC columns, as they require a special and/or large device to stretch FRP sheets. Xiao and Ma [4] suggested an external pressing method to attach a prefabricated FRP jacket on a RC column using several belts. However, they still used an adhesive on the concrete surface to bond the prefabricated FRP jacket as well as lateral band-strips to apply lateral pressure on the FRP jacket. This method was more efficient to obtain perfect attachment of the FRP sheet than the previous manual attachment methods since they apply external pressure on the FRP jackets.

Choi et al. [2,5] suggested a new steel jacketing method for RC columns, where external pressure is used to attach the steel jacket to concrete instead of grouting. The effectiveness of the jacketing

* Corresponding author. Tel.: +1 404 895 5241; fax: +1 404 894 1641.
E-mail addresses: eunsoochoi@hongik.ac.kr (E. Choi), jongsu.jeon@gatech.edu (J.-S. Jeon), civcho@inje.ac.kr (B.-S. Cho), k-park@yonsei.ac.kr (K. Park).
[1] Tel.: +82 2 320 3060; fax: +82 2 332 1244.

0141-0296/$ - see front matter © 2013 Elsevier Ltd. All rights reserved.
http://dx.doi.org/10.1016/j.engstruct.2013.05.019

method was proved through the experimental tests of concrete cylinders and RC columns. The method is similar to Xiao and Ma's method and the perfect attachment is critical to obtain satisfactory performance. Harries and Kharel [6] and Harries and Carey [3] noted the presence of a gap between the concrete and the confining jacket due to the slackness in the confinement and explained the effect of the gap. They also indicated that the behavior of woven fabric was similar to that of the gap. As presented in the aforementioned studies, overcoming the problem of the gap or the slackness of the jackets of steel plate or FRP fabrics is challenging. This study sheds light on the advantages of wire-type jackets for confining concrete structures without a gap or slackness.

2. FRP wire jacket and specimens

2.1. FRP wire jacket

Glass-fiber reinforced polymer (GFRP) wire of 1.0 mm diameter was used in this study. The area of the wire was 0.785 mm^2 and the tensile strength and ultimate strain of the wire were 1230.6 MPa and 2.94×10^{-2}, respectively. Therefore, the estimated Young's modulus in tension was 41.84 GPa. Firstly, the wire was wound around a large reel, as shown in Fig. 1a, and the reel was equipped with a device to provide friction resistance at its side when rolling. The wire was stretched over a concrete cylinder on a special device manufactured for this study, as shown in Fig. 1b. The device held a concrete cylinder and wrapped the wire around the cylinder with a specific pitch. Note that no adhesive was applied on the concrete surface. During the winding, the wire was stretched with a constant tension because of the frictional resistance of the reel. Tensile force of 25 N was measured using a spring balance, as shown in Fig. 1c and d. Therefore, the stress and strain in the wire due to the tensile force were 31.83 MPa and 7.73×10^{-4}, respectively. The stress was too small to develop an active confining effect on the concrete but sufficient to tightly wind the wire on the concrete surface without any gap. After several windings of the wire, super glue was applied on the wire to prevent release of the wire during the rolling. After finishing the winding, super glue was also applied on the wire at the other side. The glue provided holding action for the wire and prevented release of the wire. Fig. 2 shows the process of confining the concrete cylinder by the FRP wire jacket. Several previous studies of shape memory alloy (SMA) wire jackets were conducted [7–10] and have used anchoring nails to hold SMA wire. The FRP wire jacket, however, can be fixed by applying glue at both ends and does not make any scar on the concrete surface. A 10 mm section of the cylinder at both ends was not wrapped by the FRP wire in order to avoid interaction of the FRP wire jacket during a compressive test. The proposed jacketing method can wrap a concrete cylinder with multiple layers; the second layer of the jacket can be built following the same procedure as used for the first layer. Fig. 3 shows the cases of single-, double-, and triple-layered FRP wire jackets and an epoxy applied specimen.

2.2. Specimens and test set-up

This study used concrete cylinders with a diameter of 150 mm and height of 300 mm to obtain the compressive behavior of confined concrete. Two variables were considered, peak strength of concrete and amount of confining FRP wire; three design strengths of concrete and three amounts of FRP wire were also considered. The design strengths were 25, 35, and 45 MPa, respectively, and the amounts of FRP wire were one, two, and three layers. The volumetric ratio for the FRP wire jacket can be calculated using the following equation:

$$\rho_v = \frac{4A_j}{sD} \tag{1}$$

where A_j = cross-sectional area of the jacket, D = diameter of cylinder, and s = spacing between wires. The calculated volumetric ratios for each amount of FRP wires were 2.09%, 4.19%, and 6.28%, respectively. To obtain an equivalent thickness of FRP sheet jackets which

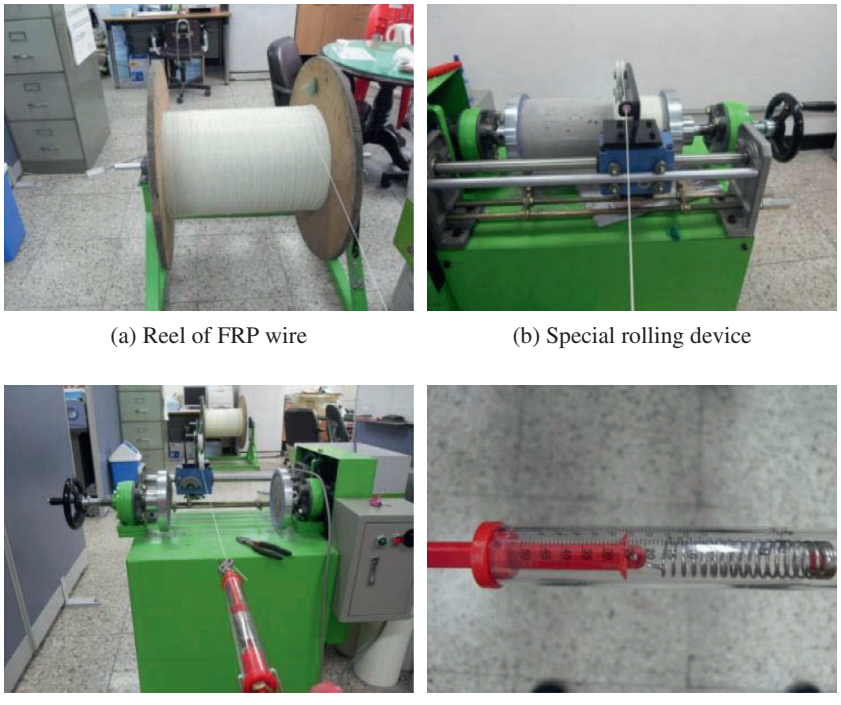

(a) Reel of FRP wire (b) Special rolling device

(c) Measuring tensile force of the wire (d) 25 N tensile force

Fig. 1. FRP wire and tensile force.

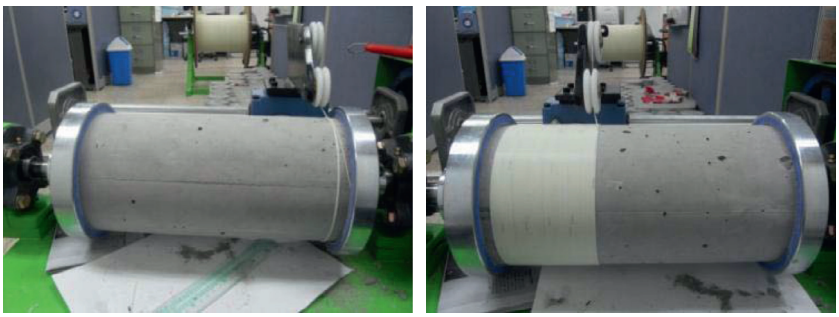

(a) Starting of rolling (b) Rolling wire

(c) Complete rolling (d) Jacketed specimen

Fig. 2. FRP wire rolling procedure.

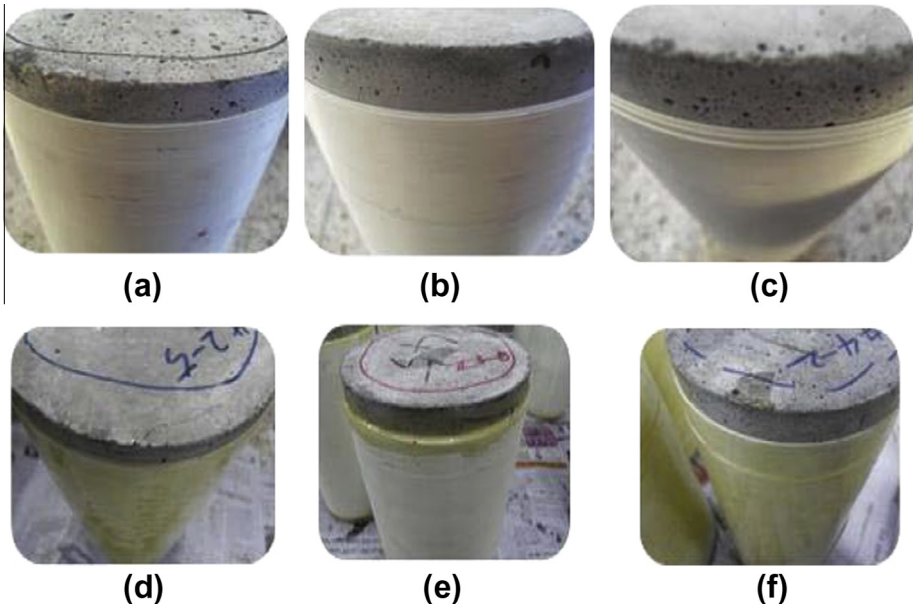

Fig. 3. Types of specimens: (a) single layer, (b) double layer, (c) triple layer, (d) epoxy application, (e) non-epoxy application, and (f) partial jacket.

have the same volumetric ratios of the FRP wire jackets, the below formulation can be used:

$$\rho_v = \frac{4t_j}{D} \tag{2}$$

where t_j = thickness of FRP sheet jacket. Therefore, the matching thickness is 0.785 mm for 1.0 mm diameter wire.

The pitch from center to center for all specimens was 1.0 mm and any gap between wires did not exist. Three specimens were prepared for each case and a total of 36 specimens including nine plain specimens were prepared. Epoxy was applied on the outer surface of FRP wire for two out of three specimens in each case. The epoxy was expected to provide shear resistance between wires and restrain the relative movement of the wires. For the remaining one specimen in each case, both ends of 5 mm length were applied with epoxy over the super glue to provide sufficient holding. The last variable was a partially wrapped jacket; the first layer was wrapped fully from top to bottom, whereas the second was wrapped partially at the middle of the specimen with a length of 180 mm or 230 mm. The bulge of the concrete cylinder during the compressive test occurs mainly at the middle and the wire at both ends may not provide significant passive confining pressure.

For partial jackets, three cylinders of 35 MPa were used for each case. Table 1 shows the test matrix of this study.

The tests were conducted with displacement controlled monotonic loading. For the test, two sole plates were placed at the top and bottom of each specimen, and three displacement transducers with a 120° angle were placed between the plates to measure axial deformation of the specimen. Furthermore, an extensometer with a gage length of 100 mm was installed at the middle of the specimen to achieve the axial deformation of the specimen. Finally, an extensometer was installed in the lateral direction to measure the circumferential deformation of the specimen. Fig. 4 illustrates the test set-up used in this study.

3. Test results of full jacketed specimens

3.1. Axial behavior

In the initial loading step, the axial deformation measured by displacement transducers may be overestimated due to a contact problem between the sole plate and the concrete surface. When the contact is not perfect in the beginning, the stress–strain curve consequently shows a much smaller slope than the actual slope. The deformation from initial to peak strength was therefore measured by an extensometer. However, after the peak strength, the FRP wire did not show composite behavior with the inner concrete, because slipping between the FRP wire and concrete occurred with increasing deformation. Therefore, after the peak strength, the deformation measured by the displacement transducer was used to draw the axial stress–strain curve of the specimen, since the sole plates contacted the concrete surface perfectly and the measured displacement thus reflects the deformation of the concrete cylinder precisely.

Fig. 5 shows the axial stress–strain curves of the confined specimens compared with those of the plain specimens. Table 2 also illustrates the corresponding peak strength and the ultimate strain, which indicates the failure-point of the FRP wire. In the table, "F" and "P" denote full and partial jacket, respectively. The number in the middle indicates the layer number or the length of the partial jacket. "N" and "E" denote non-epoxy and epoxy application. The average peak strength and the corresponding strain of plain concrete specimens are presented in the table. The average peak strengths for 25, 35, and 45 MPa specimens were 36.1, 47.2, and 57.1 MPa, respectively. The corresponding strains at peak strength varied from 2.28×10^{-3} to 2.57×10^{-3}.

The axial stress–strain curves of the concrete confined by the FRP wire jacket showed bilinear behavior with a transition region, corresponding exactly with the axial behavior of concrete confined by FRP sheets or tubes. In general, more confinement increased the peak strength and failure strain. In each suite of specimens, the strength ratio (f'_{cc}/f'_{co}) increased with more use of FRP wire, and the relationship between the two parameters was almost linear. However, there were two remarkable observations: (1) softening behavior was observed after the peak strength and hardening behavior appeared following the softening and (2) strength degradation appeared approaching the failure point.

Csuka and Kollar [11] indicated that the softening and following hardening behavior of confined concrete after the peak strength are related to the stiffness ratio of the confining stiffness to that of unconfined concrete. The confining pressure of the FRP-wire jacket is calculated as given below.

$$f_l = \frac{2f_j A_j}{sD} = \frac{2E_j \varepsilon_j A_j}{sD} \tag{3}$$

where f_j = hoop stress in the jacket, E_j = elastic modulus of the wire, ε_j = ultimate strain of the wire, A_j = cross-sectional area of the jacket, D = diameter of cylinder, and s = spacing between wires (s = 1 mm in this study). In the above equation, the remaining part excluding ε_j is the stiffness of the jacket in the circumferential direction. Therefore, the stiffness ratio, ρ_s, is defined as:

$$\rho_s = \frac{2E_j A_j}{sDE_c} \tag{4}$$

where E_c is the elastic modulus of unconfined concrete; this study adopted a value of $4750\sqrt{f'_{co}}$ recommended by ACI 318M-02 [12]. The calculated stiffness ratios of the confined concrete are shown in Table 3. Csuka and Kollar [11] argued that the softening and following hardening were due to the low stiffness of the jacket. For higher stiffness, the stress–strain curves were monotonically increasing. Based on this observation, the single-layered jackets for all types and the double-layered jacket for the 45 MPa specimen were low stiffness jackets. They also proposed a limit on the stiffness ratio of a low stiffness jacket as follows:

$$\rho_{s,limit} = \begin{cases} 0.0195 + \frac{f'_{co}-40}{3100}, & \text{if } f'_{co} \leqslant 40 \text{ MPa} \\ 0.0195 + \frac{f'_{co}-40}{12{,}000}, & \text{if } f'_{co} \geqslant 40 \text{ MPa} \end{cases} \tag{5}$$

The calculated limits of the low stiffness ratio were 0.01824, 0.0201, and 0.0209 for the 25F, 35F, and 45F specimens, respectively. Comparing the stiffness ratio limits to the values in Table 3, Eq. (5) worked well for the 25 and 35 MPa specimens; the specimens with smaller stiffness ratios than the limit showed softening and hardening, and the specimens with larger stiffness ratios than the limit showed monotonically increasing behavior. However, for the 45F specimen, the stiffness ratio of the double-layered specimen (0.0244) was larger than the limit (0.0209), but two of the three specimens showed softening and hardening behavior, although the degree was much smaller than that of the single-layered specimens. Therefore, in general, the axial stress–strain behavior of the FRP-wire confined concrete corresponded to the observations of Csuka and Kollar [11].

Csuka and Kollar also investigated the effect of the confinement ratio on the axial stress–strain curve. The confinement ratio (ρ_c) of the confined specimens was calculated using the following equation:

$$\rho_c = \frac{f_l}{f'_{co}} \tag{6}$$

Table 1
Test matrix.

Types	25 MPa		35 MPa		45 MPa		
	Epoxy	Non-epoxy	Epoxy	Non-epoxy	Epoxy	Non-epoxy	
Full jacket							
Single	2	1	2	1	2	1	Three specimens for each design strength
Double	2	1	2	1	2	1	
Triple	2	1	2	1	2	1	
Partial jacket							
180 mm			2	1			
230 mm			2	1			

(a) Non-epoxy applied specimen (b) Epoxy-applied specimen

Fig. 4. Test set-up for axial compressive test.

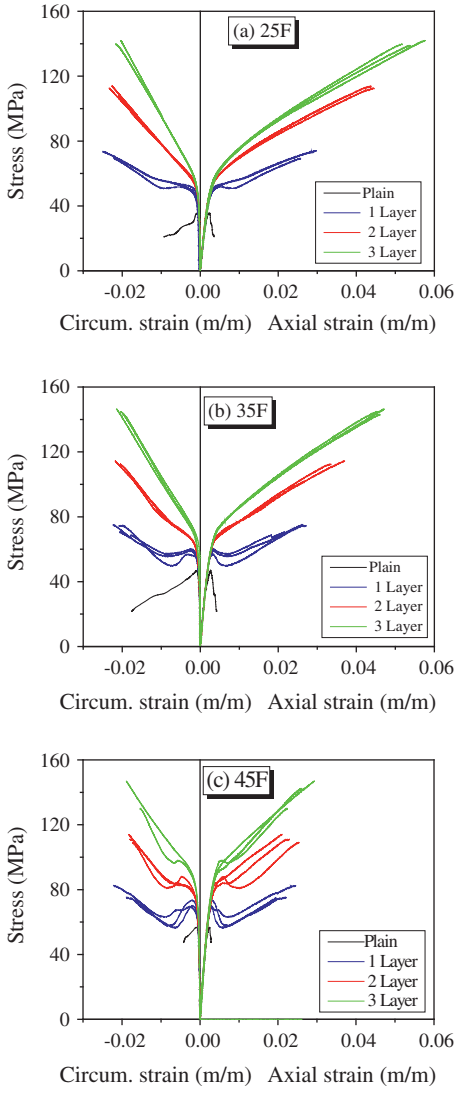

Fig. 5. Stress–strains curves of confined specimens in axial and circumferential direction.

Table 2
Peak strength and ultimate strain of confined specimens.

Type	f'_{cc} (MPa)	ε_f (%)	f'_{cc}/f'_{co}	$\varepsilon_{f,cir}$ (%)	Plain concrete
25F-1-1E	73.92	2.97	2.05	2.65	$f'_{co} = 36.08$ MPa
25F-1-2E	73.15	2.89	2.03	2.49	$\varepsilon_{co} = 2.57 \times 10^{-3}$
25F-1-3N	69.27	2.57	1.92	2.21	
25F-2-1E	112.5	4.45	3.12	2.32	
25F-2-2E	113.8	4.38	3.15	2.26	
25F-2-3N	110.0	4.02	3.05	2.08	
25F-3-1E	138.9	5.40	3.85	2.13	
25F-3-2E	139.8	5.18	3.87	2.17	
25F-3-3N	141.2	5.76	3.91	2.03	
35F-1-1E	75.00	2.63	1.59	2.23	$f'_{co} = 47.16$ MPa
35F-1-2E	74.64	2.73	1.58	2.09	$\varepsilon_{co} = 2.52 \times 10^{-3}$
35F-1-3N	70.55	2.16	1.50	2.07	
35F-2-1E	114.3	3.70	2.42	2.18	
35F-2-2E	101.4	2.67	2.15	1.69	
35F-2-3N	112.4	3.36	2.38	2.04	
35F-3-1E	146.5	4.72	3.11	2.14	
35F-3-2E	142.9	4.61	3.03	1.98	
35F-3-3N	144.9	4.54	3.07	2.04	
45F-1-1E	75.16	2.20	1.32	1.89	$f'_{co} = 57.10$ MPa
45F-1-2E	82.44	2.45	1.44	2.22	$\varepsilon_{co} = 2.28 \times 10^{-3}$
45F-1-3N	74.81	1.95	1.31	1.67	
45F-2-1E	109.0	2.54	1.91	1.73	
45F-2-2E	111.0	2.30	1.94	1.79	
45F-2-3N	113.9	2.10	1.99	1.83	
45F-3-1E	146.9	2.93	2.57	1.89	
45F-3-2E	142.1	2.61	2.49	1.62	
45F-3-3N	131.4	2.59	2.30	1.76	

Table 3
Stiffness and confinement ratios of confined concrete.

Type	25 MPa	35 MPa	45 MPa
f'_{co} (MPa)	36.1	47.2	57.1
E_c (MPa)	28539.6	32633.6	35893.2
Stiffness ration (ρ_s)			
1 Layer	0.0153	0.0134	0.0122
2 Layer	0.0307	0.0268	0.0244
3 Layer	0.0460	0.0402	0.0366
Confinement ratio (ρ_c)			
1 Layer	0.3568	0.2729	0.2256
2 Layer	0.7136	0.5458	0.4511
3 Layer	1.0704	0.8187	0.6767

It is clear from Table 3 that a lower confinement ratio produced more noticeable softening/hardening behavior. However, Csuka and Kollar [11] showed that different stiffness ratios produced monotonic or softening/hardening behavior despite that they had the same confinement ratio. In relation to the confinement ratio, several previous studies have raised the issue of insufficient con-

finement. Mirmiran et al. [13] reported that the stress of confined concrete at the ultimate strain falls below f'_{co} when the confinement is insufficient. The criterion for a circular specimen was $f_l/f'_{co} < 0.15$. Later, Spoelstra and Monti [14] suggested a lower value, $f_l/f'_{co} < 0.07$, using their analysis-oriented model. In Table 3, all confinement ratios were larger than both criteria, and all curves in Fig. 5 showed larger ultimate strengths than the unconfined peak strength. The confined concrete specimens in this study thus had sufficient confinement, although a few specimens had low stiffness.

The bulge of the concrete cylinder in the lateral direction varied according to the height of the specimen, indicating that the developed stresses in the wires were different. If the difference in the stress between two adjacent wires became larger than the frictional resistance of the concrete surface to the movement of wires, stress redistribution might occur. The wire-stress at the middle of the specimen would then decrease and the strength increment would be weakened. Strength degradation did not occur for the concrete confined by FRP sheets or tubes, however, as the stress redistribution was not observed.

The application of epoxy provided shear resistance between the wires and prevented stress redistribution between wires. Therefore, the epoxy applied specimens were expected to show larger peak strength than the non-epoxy applied specimens. This hypothesis was clearly verified for the single layered specimens of 25F and 35F: the epoxy applied specimens showed 6% larger peak strength than the non-epoxy applied specimens. However, the hypothesis was not suitable for the cases of high strength concrete and/or multi-layered confinement. For the multi-layered jackets, inner wires were subjected to pressure from the outer wires, and stress redistribution was impeded. For high strength concrete, the failure strains of FRP wires were relatively small compared with those of low or middle strength concrete, and the wire-stress at the middle of the specimen did not fully reach the ultimate strain. It appears that the early failure of FRP wires did not produce a sufficient stress-difference between wires to generate stress redistribution.

3.2. Circumferential and volumetric behavior

Circumferential strain was estimated by dividing the measured circumferential deformation by the perimeter of a specimen. The curves of axial stress versus circumferential strain are shown in Fig. 5. The curves also showed bilinear behavior except for the case of the softening/hardening behavior; this was similar to the behavior of concrete confined by a FRP sheet or tube.

The failure strains in the circumferential direction, as indicated in the fifth column of Table 2, generally decreased with increasing amount of FRP-wire confinement. In addition, the circumferential failure strains were smaller than the ultimate tensile strain of the FRP wire; this also corresponded to previous studies of FRP sheet or tube confinement. The circumferential failure strain showed a tendency to decrease with increasing confinement and peak strength of the unconfined concrete, and the ratios of the circumferential failure strain to the ultimate tensile strain of the FRP-wire ranged from 55% to 90%. Xiao and Wu [15] conducted compressive tests of concrete confined by FRP sheets and indicated that the circumferential failure strains were approximately 50–80% of the rupture strains obtained from tensile coupon tests. Lam and Teng [16] also investigated the circumferential failure strains of concrete confined by FRP sheets reported in several studies, including Xiao and Wu's study [15], and obtained a similar tendency to the above range with an average value of 63%. The present results are consistent with those of previous studies.

The epoxy application appeared to increase the circumferential failure strain for single-layered jackets due to restriction of stress redistribution. However, for multi-layered jackets, the effect was not observed clearly. As previously mentioned, for multi-layered jackets, the inner jacket was pressured by the outer jackets, which prevented stress redistribution.

The volumetric strain of concrete during the compressive test of a cylinder can be calculated using the axial and circumferential strain as follows:

$$\varepsilon_{vol} = \varepsilon_1 + \varepsilon_2 + \varepsilon_3 = \varepsilon_{axial} + 2\varepsilon_{cir} \tag{7}$$

where ε_1 is the axial strain, and ε_2 and ε_3 are lateral strains in the lateral directions, which are the same as the circumferential strain. When ε_1 takes a positive sign and the others are negative, volumetric strain ε_{vol} is positive for a volume reduction (compaction) or negative for a volume increase (dilation). It is well known that the volumetric strain of unconfined concrete shows compaction almost linearly up to 75–90% of the peak strength. At this point the direction of the volume change is reversed, resulting in a volumetric expansion near or at the peak strength. For confined concrete, Samaan et al. [17] compared the volumetric behaviors of FRP-confined and steel-confined concrete. They indicated that steel-confined concrete showed abrupt volume expansion with yielding of steel. However, for FRP-confined concrete, the volumetric behavior is totally different from that of steel-confined concrete, since the circumferential stress of the FRP increases linearly up to its rupture point. Mirmiran and Shahawy [18] measured the volumetric response of FRP-confined concrete with varying amounts of FRP confinement and indicated that lateral expansion of concrete can be effectively diminished with an adequate amount of FRP confinement.

The volumetric strains of full FRP wire-confined concrete are shown in Fig. 6 with the normalized axial stress f'_{cc}/f'_{co}, which is the ratio of the peak strength of confined concrete to that of unconfined concrete. In Fig. 6a, for the 25F specimen, the volumetric strain of the single-layered specimen changed from compaction to dilation at an axial stress above the peak strength of unconfined concrete, and the dilation increased continuously until failure. The double-layered specimen reversed the dilation but failed in the expansion region. However, the triple-layered specimen curtailed the expansion of volume effectively, as also reported by Mirmiran and Shahawy [19], and the dilation was reversed at a normalized axial stress of approximately 2.1. The specimen failed in the compaction zone. However, the triple-layered specimen in the 35F specimens permitted slightly more dilation, although it reversed the dilation. In addition, in the 45F specimen, the triple-layered specimen failed to control the expansion of volume. It was observed that the same amount of FRP wire confinement showed different volumetric behavior according to the type of concrete. Therefore, the volumetric behavior of confined concrete was affected by properties of the concrete and external jacket. To explain this, Mirmiran and Shahawy [18] introduced the stiffness ratio, which has been defined already in the above. However, they used f'_{co} instead of E_c, since E_c is a function of f'_{co}. This study used the stiffness ratio defined in Eq. (4). When a stiffness ratio of a FRP wire jacket was relatively small, the volume of the specimen expanded until it was failed. However, the sufficiently large stiffness ratio restricted the volume expansion. For 25F specimens in Fig. 6a, the single-layered specimen increased volumetric strain until its failure while the triple-layered specimen effectively restrained the volume expansion. In Fig. 6, the double-layered jacket of 25F and 35F specimens reversed the volume expansion but did not enter contraction zone at failure; for the two cases, the stiffness ratios were 0.031 and 0.027, respectively. Additionally, the triple-layered 45F specimen showed the similar behavior as other 45F specimens with the stiffness ratio of 0.037. The triple-layered 35F specimen has the lowest stiffness ratio of 0.04 associated with the effective restriction of the volume expansion. From the observation, it appears that a marginal stiffness ratio for restraining volume-expansion ranges between 0.037 and 0.04. The specimens with a double-

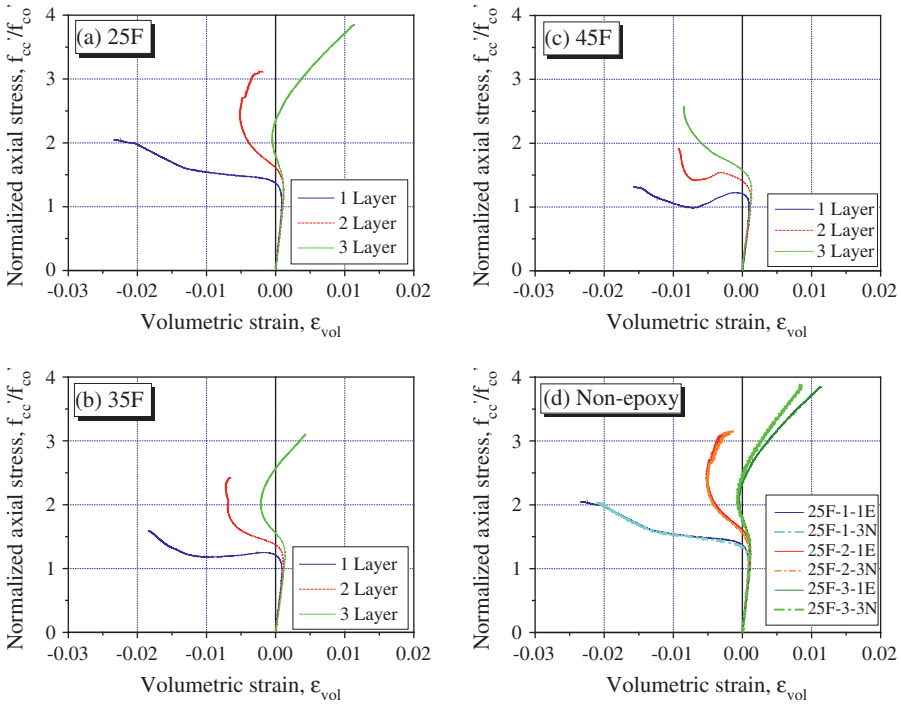

Fig. 6. Volumetric behavior of FRP wire-confined concrete.

layer of 25F and 35F and a triple-layer of 45F, respectively, had high stiffness ratios but failed to restrict the volumetric expansion. The stiffness ratio limit for restraining volumetric expansion has not yet been investigated and further study is required.

The volumetric behaviors of epoxy applied specimens are compared with those of non-epoxy applied specimens in Fig. 6d. For the single and double-layered specimens, the epoxy applied and non-epoxy specimens showed almost the same behavior. For the triple-layered specimen, the epoxy applied specimen showed somewhat effective compaction at around the failure point. In general, epoxy application on the outer surface of the FRP-wire jacket appeared not to significantly affect the volumetric behavior of FRP-wire confined concrete.

3.3. Failure mode

The FRP wire-confined concrete cylinders showed different types of wire-fracture according to the application of epoxy as shown in Fig. 7. When epoxy was applied on the outer surface of the FRP wire, a bundle of wires at the mid-height of the specimen was fractured simultaneously due to circumferential tension (see Fig. 7a). This is the most common failure mode for concrete confined by FRP sheets [16,20]. For non-epoxy application, the single-layer wire fractured at a single point and unfastened (see Fig. 7b). However, for multiple layers, the wire fractured at multi-points simultaneously at the mid-height of the specimen (see Fig. 7c), since the specimen failed abruptly due to expansion at the mid-part.

Fig. 8 shows the failure types of interior concrete. These are classified into two categories: (1) the crushing at the mid-part without separation into several parts: and (2) fracture with large horizontal cracks including crushing at the mid-part. The first type corresponded to the class of specimens with softening/hardening behavior. In this case, the failure of concrete occurred at the local maximum point of the curves, and the concrete was totally crushed at the local minimum point. After that, the hardening behavior was due to the elasticity of the FRP wire. However, for the second type, the failure of concrete occurred at the end of the transition of the

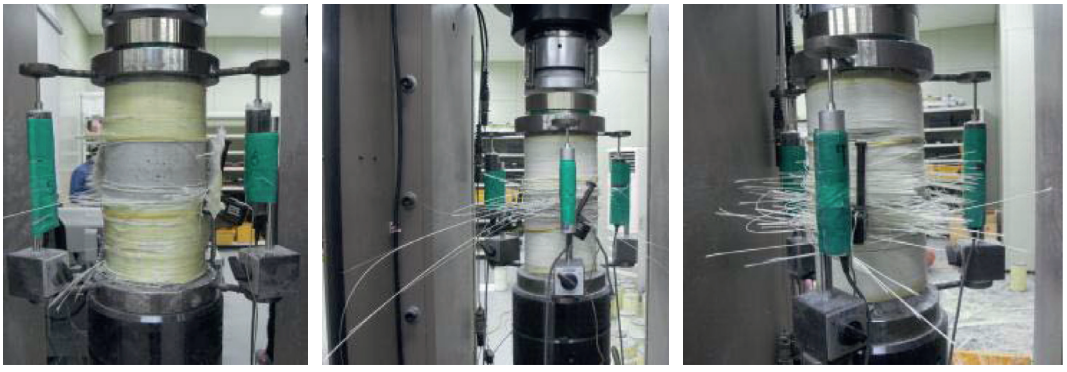

(a) 45F-1-1E (b) 25F-1-3N (c) 45F-3-3N

Fig. 7. Fracture-types of FRP wire jacketed specimens.

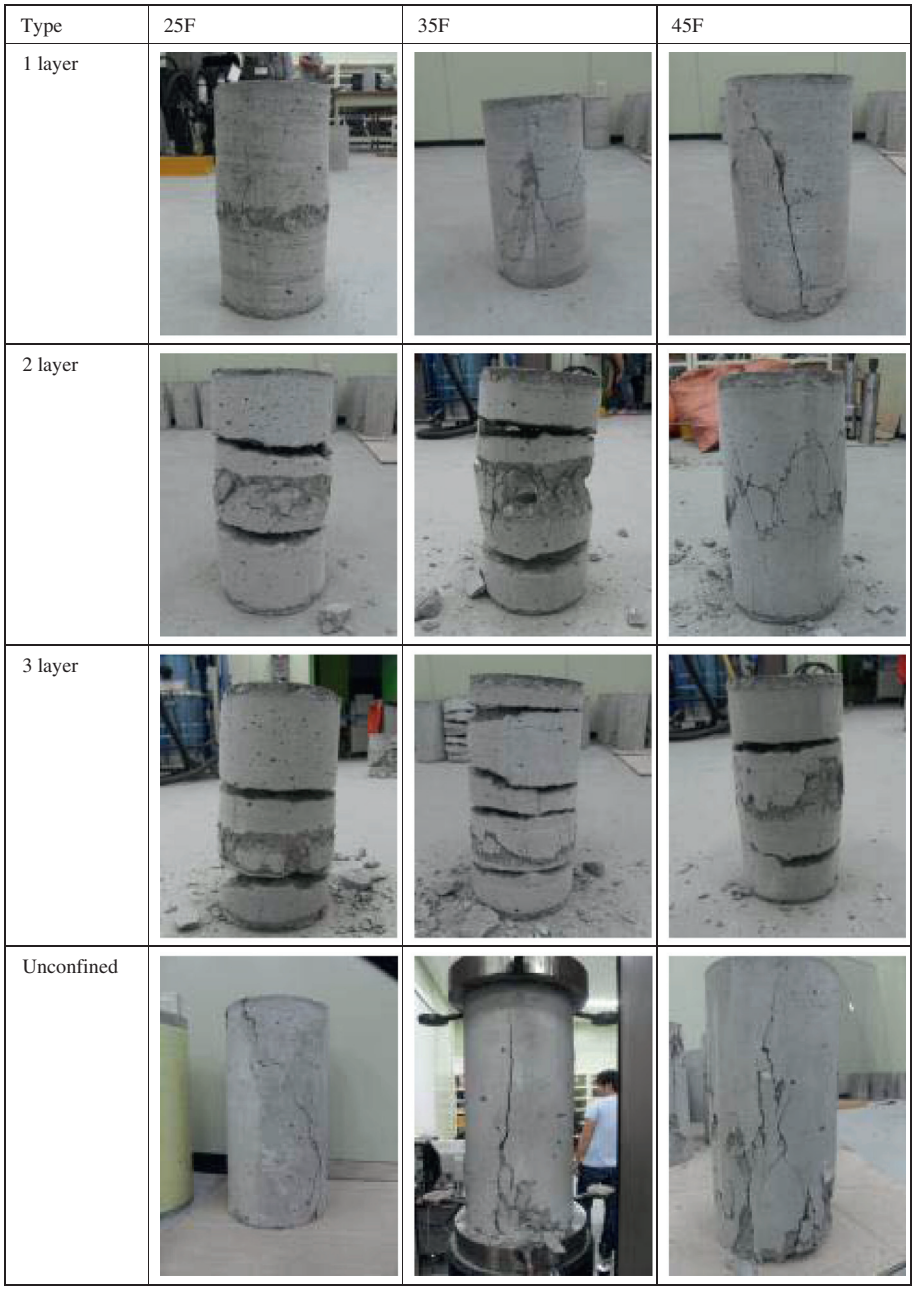

Fig. 8. Failure types of inside concrete.

curves, and the interior concrete was confined effectively by the FRP wire jacket. Then, the FRP wire jackets fractured abruptly at the mid-part, and the concrete at this region then expanded abruptly, which caused contraction in the axial direction due to Poisson's effect and large horizontal cracks. The second failure type occurred in the specimens in which volumetric expansion was restrained effectively. Therefore, the failure type of interior concrete appeared to be related to the stiffness ratio. For the second case, another presumption is possible. These horizontal cracks were caused by shearing which developed from sudden expansion of the concrete due to confinement ruptures at one side while the FRP jacket was still working in hindering expansion of concrete at the other side of the crack.

The single-layered specimen of 45F with a low stiffness ratio showed a large diagonal crack that was similar to the crack pattern of the unconfined concrete. The diagonal or vertical crack disappeared with increasing stiffness ratio, and mid-part crushing developed.

3.4. Partially jacketed specimens

The stress–strain curves for partially jacketed specimens in the axial and circumferential directions are shown in Fig. 9. Additionally, the figure presents a comparison of volumetric strains between fully and partially jacketed specimens. The corresponding values are presented in Table 4. The peak strengths of the partially jacketed specimens were smaller than those of the fully jacketed specimens. For the 230 mm case, the average peak strength was 94.8% of that of the fully jacketed specimens, and the value for the 180 mm case was 68.1%. Also, the percentage of ultimate strains was 76.9% and 71.0% for the 230 and 180 mm cases, respectively, compared to the full-jacket case. In Fig. 9a, the 230 mm jack-

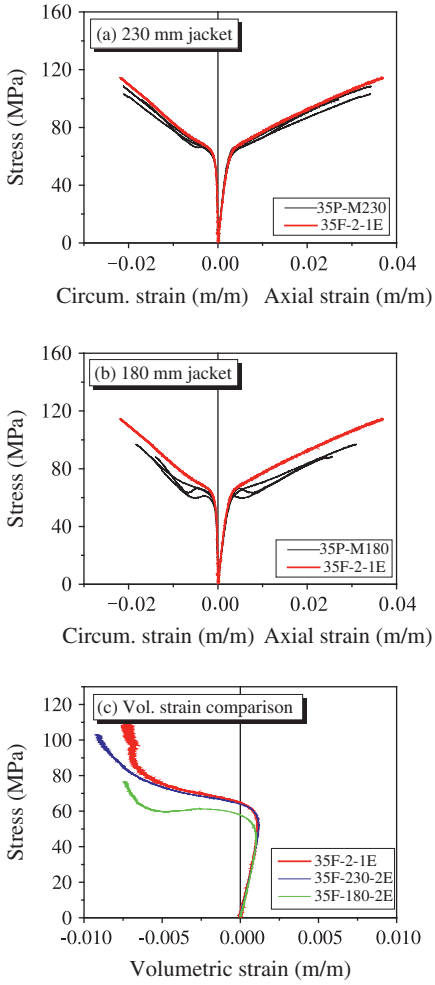

Fig. 9. Axial, circumferential, and volumetric behavior of partially jacketed specimens.

Table 4
Peak strength and ultimate strain of partially jacketed specimens.

Type	f'_{cc} (MPa)	ε_f (%)	f'_{cc}/f'_{co}	$\varepsilon_{f,cir}$ (%)	Plain concrete
35P-230-1E	99.11	2.71	2.10	1.69	$f'_{co} = 47.16$ MPa
35P-230-2E	108.3	2.46	2.30	2.11	$\varepsilon_{co} = 2.52 \times 10^{-3}$
35P-230-3N	103.2	2.31	2.19	2.12	
35P-180-1E	87.93	2.44	1.86	1.40	
35P-180-2E	88.25	2.56	1.87	1.50	
35P-180-3N	96.93	1.89	2.06	1.84	

et specimens followed the equal path of the fully jacketed specimen up to the beginning of the transition zone. However, the slope of the second linear zone was slightly smaller than that of the fully jacketed specimen. This means that the 230 mm jacket was less effective in terms of confining concrete after the transition zone, with propagation of a dilation region toward the ends of the specimen. The 180 mm jacketed specimens showed smaller stress at the transition zone than that of the fully jacketed specimens as well as the softening and subsequent hardening behavior mentioned previously. The cause of the two observations was the relatively low stiffness ratio of the 180 mm jacketed specimens. Fig. 10 shows the failure modes of the partially jacketed specimens. The 180 mm jacket fractured at the end of the specimen including the junction region of the partial jacket. Therefore, the stress started to decrease at an earlier time point than for the fully jacketed specimen, and failure at the end zone also occurred earlier; these two factors caused a drastic decline of the peak strength. For the 230 mm jacket case, the initial decrease of the stress did not occur. However, the fracture developed around the mid-height of the specimen including the junction of the partial jacket, resulting in earlier fracture. Therefore, the 230 mm jacketed specimen showed similar peak strength to that of the fully jacketed specimen. The volumetric strain curve for the 230 mm jacket specimen followed the curve for the full-jacket specimen after the transition zone but showed slightly larger expansion at around the failure point. However, the 180 mm jacket specimen expanded at smaller stress as compared to the full or the 230 mm jacket specimen. Therefore, the 180 mm jacket did not restrain the expansion of concrete in the first linear zone, as shown in Fig. 9c.

4. Analysis of confinement effectiveness

4.1. Confinement effectiveness

Most of the existing models to estimate peak strength of confined concrete have adopted the following form:

$$\frac{f'_{cc}}{f'_{co}} = 1 + k_1 \frac{f_l}{f'_{co}} \tag{8}$$

where k_1 is the confinement effectiveness coefficient. The equation was first suggested by Richart et al. [21], and Fardis and Khalili [22] noted that the model could be used for FRP-confined concrete. Richart et al. [21] estimated a k_1 of 4.1 for actively confined concrete, and Miyauchi et al. [23] reported a k_1 of 2.98 for FRP-confined concrete; in the models, k_1 was a constant. In other models, k_1 was a function of f_l/f'_{co} [24–26] or f_l [17]. This study adopted the model with a constant k_1, since the model is simple and favorable to compare the confinement effectiveness of the FRP wire jacket with the results of other studies.

Table 3 and Fig. 11 show the calculated confinement ratios and the regression results, respectively, for all specimens. Comparing the confinement effectiveness according to the peak strength of unconfined concrete, the values of k_1 were estimated as 2.78, 2.46, and 2.10 for the 25F-, 35F-, and 45F-specimens, respectively. Therefore, the confinement effectiveness for lower peak strength concrete was better; the k_1 value of 25F-specimen was larger by 32.5% than that of the 45F-specimen. Using all data, k_1 was estimated as 2.55. Lam and Teng [27] suggested a k_1 of 2.0 for concrete confined by FRP sheets based on a wealth of experimental data. However, the proposed value was too conservative, and the average value of the used data was 2.62 with very large scatter. Therefore, the k_1 of the FRP wire jacket in this study is similar to that of FRP sheet jackets in previous studies.

4.2. Circumferential rupture strain

In general, the rupture strains ε_{jr} of concrete confined by FRP sheets in the circumferential direction are smaller than the ultimate strains ε_{fu} obtained from tensile coupon tests; the rupture strains are approximately 60% of the ultimate strains [16]. This study observed the same phenomenon in concrete confined by a FRP wire jacket. For FRP sheet jackets, the causes were posited to be (1) stress concentration in cracked concrete leading to localized strain and premature rupture of FRP sheets [28]; and (2) the curvature effect of FRP sheets on the tensile strength of FRP. The first cause is only valid when bonding between FRP and concrete is secured. However, for the FRP wire jacket in this study, there was no epoxy between the FRP and concrete, and bonding was not provided- only friction existed between them. If the difference between the stress in cracked concrete and the stress in other parts

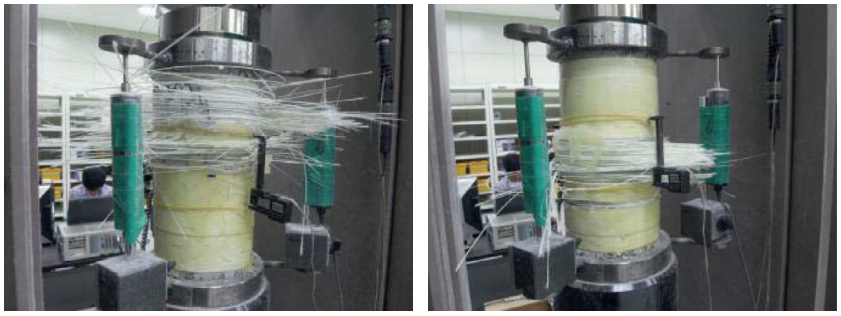

(a) 35P-180-1E (b) 35P-230-2E

Fig. 10. Failure modes of partially jacketed specimens.

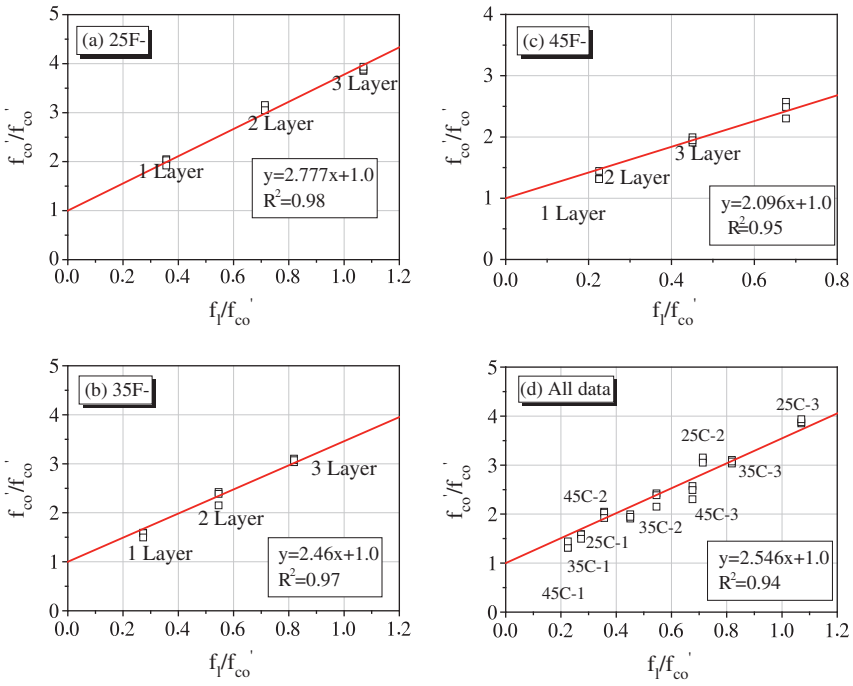

Fig. 11. Estimation of confinement effectiveness using f_l.

becomes larger than the frictional force, stress redistribution in the FRP wire occurs, which reduces the peak stress in the wire. Since the frictional force increases with increasing tensile force in FRP wire, the frictional force, after a critical point, can prohibit stress redistribution in the wire, and the wire may be ruptured due to stress concentration. Therefore, it appears that the first cause is partially valid for the FRP wire jacket. However, the second cause cannot be applied for the wire, since wire does not have bending rigidity related to curvature. It can be explained that the concrete specimen was fractured explosively and the stress was dropped suddenly; the FRP wires were fractured at the ultimate tensile strain due to the sudden expansion of the concrete; however, the stress–strain curve was truncated at the peak strength; and thus the failure strain of the FRP wire was smaller than its ultimate tensile strain. The previous study also indicated in situ properties which includes the misalignment or damage to jacket fibers during handling and lay-up; the inclusion of residual strains during lay-up resulting from flaws in the substrate concrete, uneven tension during lay-up, or temperature, creep, and shrinkage incompatibility between the concrete and FRP jacket; and the cumulative probability of weaknesses in the FRP material since jackets are much larger than tensile coupons [28]. FRP wire jackets can eliminate all the in situ properties which may induce earlier rupture of FRP sheet jackets.

Fig. 12 shows the ratio of FRP rupture strains in the circumferential direction to the ultimate strain of the FRP wire. The rupture strains decreased with increasing amount of FRP wire and the peak strength of unconfined concrete. The range varied from 55% to 90%, and the average of all data was 69.5%, which is slightly larger than the corresponding value of concrete confined by FRP sheet jackets. When the ratios were displayed with confinement ratios, a large scatter was observed, which corresponded to the results for FRP sheet jackets [16].

Based on the above observations, Lam and Teng [16] suggested the use of the actual confining pressure $f_{l,a}$ to estimate the confinement effectiveness in Eq. (6); $f_{l,a}$ was calculated using the FRP rupture strains measured from experimental tests. Fig. 13 shows the regression results for each type of specimen and data of all specimens. The values of k_1 were 3.82, 3.65, and 3.51 for the 25F, 35F, and 45F specimens, respectively. k_1 for all data was estimated as 3.71. Lam and Teng [16] indicated that k_1 increased to 3.3 from 2.0 for FRP sheet jackets when the actual confining pressure was used. Therefore, the k_1 value of 3.71 for the FRP wire jacket was close to that of the FRP sheet jacket. In Fig. 13, the difference be-

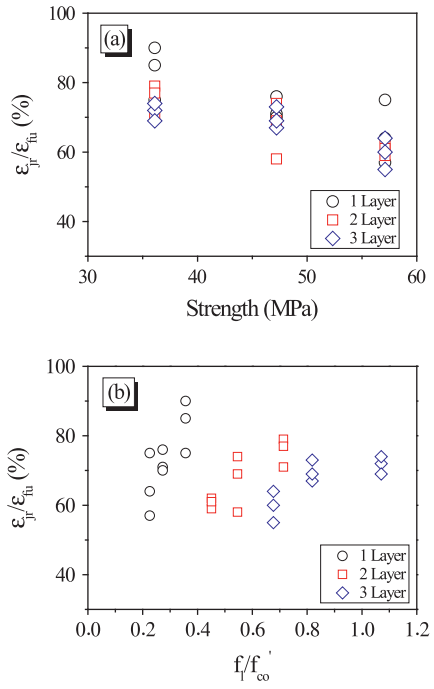

Fig. 12. Ratio of rupture strain of confined concrete in circumferential direction to ultimate strain of FRP wire as function of (a) peak strength of unconfined concrete and (b) confinement ratio of confined concrete.

tween the k_1 s of the 25F and 45F specimens was 8.7%; the corresponding value in Fig. 11 was 32.5% using the ultimate strain of the FRP wire. This indicated that the actual confinement effectiveness was the same regardless of the peak strength of unconfined concrete.

5. Discussion and applicability

The general behavior of concrete confined by a FRP wire jacket was similar to that of concrete confined by a FRP sheet jacket. However, the installation method of the FRP wire jacket was different from that of the FRP sheet jacket. The FRP sheet jacket should be attached on concrete using an adhesive such as epoxy, which induces bonding action between FRP and concrete. In this case, stress concentration in the FRP sheet developed in the vicinity of cracked concrete. For the FRP wire jacket, the wire is stretched with a small amount of tensile force and is wrapped around concrete without the use of adhesive. This process can be conducted manually or by a special machine which is similar to a yarn roller. Both cases are easier than the attachment of FRP sheets on concrete with adhesive by totally man's work. Considering speed of installation and used materials, the winding method of FRP wires would be more cost-effective than attaching FRP sheets.

This study applied epoxy on the whole outer surface of the FRP wires; this aimed to prevent stress redistribution of the wires due to stress difference between wires. The stress redistribution may reduce the confining effect of the wires and this was verified through an experimental test [3]. However, as illustrated in Table 2, the epoxy application did not increase the peak strength significantly comparing with the non-epoxy application. Epoxy is temperature susceptible and the epoxy application consumes installation time and increases installation cost. Therefore, the epoxy application on the outer surface of FRP wires is not recommended.

The holding method in this study worked well for the test of concrete cylinders, since the dilation at the end of the concrete cylinder is relatively small and the developed strain in the wire is also small. Therefore, the holding action of epoxy can endure tensile force due to the compressive test. If the end of the wire is placed at the location of large dilation, the epoxy holding may fail, as shown in the partial jacket of 180 mm. In RC columns, the largest dilation develops at the bottom of the column, where the end of the wire should be placed. Therefore, the epoxy holding method may not be applicable, and other holding method should be taken into account. FRP wire can be easily wound around RC columns using a winding machine, and this method is much more effective than manual attachment of FRP sheets using an adhesive. Consequently, the FRP wire jacket appears to be very effective for circular RC columns as a seismic retrofitting scheme.

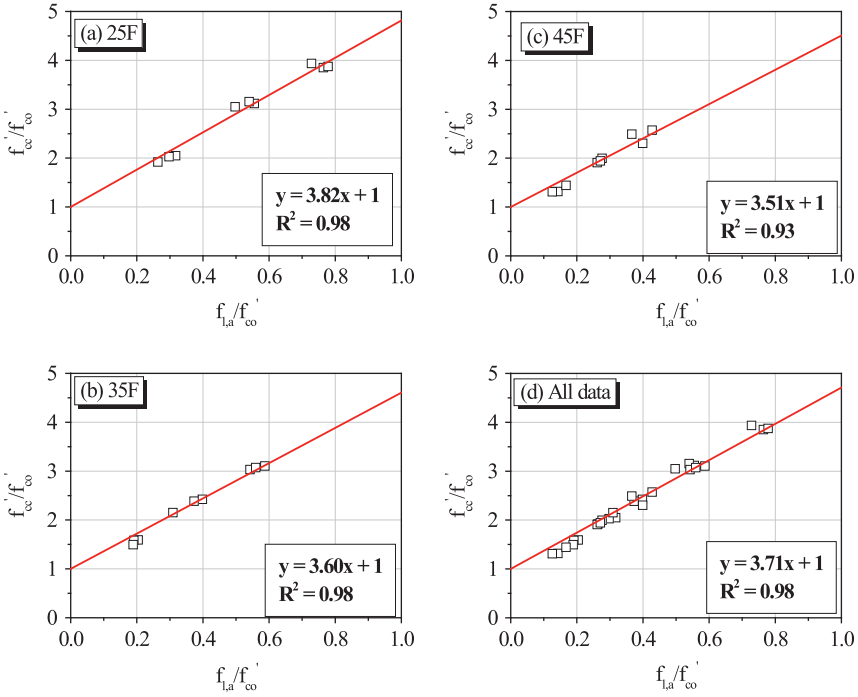

Fig. 13. Estimation of confinement effectiveness using actual confining pressure $f_{l,a}$.

6. Concluding remarks

This study proposed the use of FRP wire for external jackets of concrete and suggested an installation method to wind the FRP wire on the concrete surface. This study also conducted axial compressive tests of concrete cylinders to investigate the confining effectiveness of a FRP wire jacket with three variables: the amount of FRP wire, the peak strength of unconfined concrete, and the application of epoxy. The FRP wire jackets successfully increased the peak strength and failure strain of confined concrete. As the case of the FRP sheet confined concrete, the axial stress–strain curves of the FRP wire confined concrete showed typical bilinear behavior. However, when the stiffness ratio of the FRP wire jacket was not sufficient, the behavior showed local maximum and minimum points and, thereafter, increased the stress up to the failure point. The limit of the low stiffness ratio suggested by a previous study generally corresponded to the observations of the FRP wire confined concrete.

The rupture strain of the FRP wire jacket in the circumferential direction ranged from 55% to 90% of the ultimate strain obtained from the tensile test of the FRP wire. The observations were consistent with those of the FRP sheet jacket. This study discussed the causes of early fracture of the FRP wire based on the stress redistribution of the wire and described the volumetric behavior of FRP wire confined concrete with the stiffness ratio. It was observed that a stiffness ratio of 0.04 was a marginal value to restrain volumetric expansion.

The failure of the FRP wire confined concrete occurred at the mid-height of the cylinders and the wires at mid-height ruptured simultaneously when the epoxy was applied outside of the FRP wire. However, the wire without epoxy application fractured at a single point and released. Epoxy application on the outside surface of the FRP wire jackets did not significantly affect the behavior of the FRP wire confined concrete, although the epoxy application restrained the stress redistribution in the wire.

The partially jacketed specimens showed smaller peak strength than the corresponding fully jacketed specimens. In addition, the end of the partial jacketing portion was fractured when the length of the partial jacket was relatively small. Therefore, the partial jacket appeared to show a smaller stiffness ratio compared to the full jacket of the FRP wire.

The confinement effectiveness of the FRP wire jacket was estimated as 3.71 using the actual confining pressure, which was calculated with the actual rupture circumferential strain of specimens. The estimated value was similar to that obtained for FRP sheet jackets. The confinement effectiveness became large with smaller peak strength of concrete when the ultimate tensile strain of the FRP wire was used to calculate the lateral confining pressure of the wire. However, if with use of the actual rupture strain, the confinement effectiveness was similar regardless of the peak strength of concrete.

Acknowledgement

This study was supported by the Basic Science Research Program through the National Research Foundation of Korea funded by the Ministry of Education, Science and Technology (Project No. 2011-0023281).

References

[1] Priestley MJN, Seibel F, Calvi GM. Seismic design and retrofit of bridges. New York: John Wiley & Sons, Inc.; 1996.
[2] Choi E, Chung YS, Park J, Cho BS. Behavior of reinforced concrete columns confined by new steel-jacketing method. ACI Struct J 2010;107(6):654–62.
[3] Harries KA, Carey SA. Shape and gap effects on the behavior of variably confined concrete. Cem Concr Res 2003;33(6):881–90.
[4] Xiao Y, Ma R. Seismic retrofit of RC circular columns using prefabricated composite jacketing. ASCE J Struct Eng 1997;123(1):1357–64.
[5] Choi E, Park J, Nam TH, Yoon SJ. A new steel jacketing method for RC columns. Mag Concr Res 2009;61(10):787–96.
[6] Harries KA, Kharel G. Experimental investigation of the behavior of variably confined concrete. Cem Concr Res 2003;33(6):873–80.
[7] Choi E, Nam TH, Cho SC, Chung YS, Park T. The behavior of concrete cylinders confined by shape memory alloy wires. Smart Mater Struct 2008;17:065032.
[8] Choi E, Chung YS, Choi JH, Kim HT, Lee H. The confining effectiveness of NiTiNb and NiTi SMA wire jackets for concrete. Smart Mater Struct 2010;19:035024.
[9] Andrawes B, Shin M, Wierschem N. Active confinement of reinforced concrete bridge columns using shape memory alloys. ASCE J Bridge Eng 2010;15(1):81–9.
[10] Park J, Choi E, Park K, Kim HT. Comparing the cyclic behavior of concrete cylinders confined by shape memory alloy wire or steel jackets. Smart Mater Struct 2011;20:094008.
[11] Csuka B, Kollar LP. FRP-confined circular concrete columns subjected to concentric loading. J Reinf Plast Compos 2010;29(23):3504–20.
[12] ACI Committee 318. Building code requirements for structural concrete and commentary (ACI 318M-02). Michigan, American Concrete Institute; 2002.
[13] Mirmiran A, Shahawy M, Samaan M, El Echary H. Effect of column parameters on FRP-confined concrete. ASCE J Compos Constr 1998;2(4):175–85.
[14] Spoelstra MR, Monti G. FRP-confined concrete model. ASCE J Compos Constr 1999;3(3):143–50.
[15] Xiao Y, Wu H. Compressive behavior of concrete confined by carbon fiber composite jackets. ASCE J Mater Civ Eng 2000;12(2):139–46.
[16] Lam L, Teng JG. Design-oriented stress–strain model for FRP-confined concrete. Constr Build Mater 2003;17:471–89.
[17] Samaan M, Mirmiran A, Shahawy M. Model of concrete confined by fiber composites. ASCE J Struct Eng 1998;124(9):1025–31.
[18] Mirmiran A, Shahawy M. Dilation characteristics of confined concrete. Mech Cohes-Frict Mater 1997;2(3):237–49.
[19] Mirmiran A, Shahawy M. Behavior of concrete columns confined by fiber composites. ASCE J Struct Eng 1997;123(5):583–90.
[20] Shahawy M, Mirmiran A, Beitelman T. Tests and modeling of carbon-wrapped concrete columns. Compos Part B Eng 2000;31(6–7):471–80.
[21] Richart FE, Brandtzaeg A, Brown RL. A study of the failure of concrete under combined compressive stresses. Engineering Experiment Station, University of Illinois, Urbana, Bulletin No. 185; 1928.
[22] Fardis MN, Khalili H. FRP-encased concrete as a structural material. Mag Concr Res 1982;34(122):191–202.
[23] Miyauchi K, Inoue S, Kuroda T, Kobayashi A. Strengthening effects of concrete columns with carbon fiber sheet. Trans Jpn Concr Inst 1999;21:143–50.
[24] Karbhari VM, Gao Y. Composite jacketed concrete under uniaxial compression–verification of simple design equations. ASCE J Mater Civ Eng 1997;9(4):185–93.
[25] Saafi M, Toutanji HA, Li Z. Behavior of concrete columns confined by fiber composite. ASCE J Struct Eng 1999;124(9):1025–31.
[26] Toutanji HA. Stress–strain characteristics of concrete columns externally confined with advanced fiber composite sheets. ACI Mater J 1999;96(3):397–404.
[27] Lam L, Teng JG. Strength models for fiber-reinforced plastic-confined concrete. ASCE J Struct Eng 2002;128(5):612–23.
[28] Pessiki S, Harries KA, Kestner JT, Sause R, Ricles JM. Axial behavior of reinforced concrete columns confined with FRP jackets. ASCE J Compos Constr 2001;5(4):237–45.